Technical University of Denmark

DTU

# Multiple start codons and phosphorylation result in discrete Rad52 protein species

de Mayolo, A.A.; Lisby, M.; Erdeniz, N.; Frederiksen, Tanja Thybo; Mortensen, Uffe Hasbro; Rothstein, R.

## DTU Library
### Technical Information Center of Denmark

# Multiple start codons and phosphorylation result in discrete Rad52 protein species

Adriana Antúnez de Mayolo, Michael Lisby[1], Naz Erdeniz[2], Tanja Thybo[3], Uffe H. Mortensen[3] and Rodney Rothstein*

Department of Genetics & Development, Columbia University Medical Center, 701 West 168th Street, New York, NY 10032, USA, [1]Department of Genetics, Institute of Molecular Biology and Physiology, University of Copenhagen, Øster Farimagsgade 2A, DK-1353 Copenhagen K, Denmark, [2]Department of Molecular and Medical Genetics, Oregon Health Sciences University, 3181 SW Sam Jackson Park Road, Mail Code L103, Portland, OR 97201, USA and [3]Center for Microbial Biotechnology, BioCentrum-DTU, Technical University of Denmark, Building 223, DK-2800 Lyngby, Denmark

## ABSTRACT

**The sequence of the *Saccharomyces cerevisiae* *RAD52* gene contains five potential translation start sites and protein-blot analysis typically detects multiple Rad52 species with different electrophoretic mobilities. Here we define the gene products encoded by *RAD52*. We show that the multiple Rad52 protein species are due to promiscuous choice of start codons as well as post-translational modification. Specifically, Rad52 is phosphorylated both in a cell cycle-independent and in a cell cycle-dependent manner. Furthermore, phosphorylation is dependent on the presence of the Rad52 C terminus, but not dependent on its interaction with Rad51. We also show that the Rad52 protein can be translated from the last three start sites and expression from any one of them is sufficient for spontaneous recombination and the repair of gamma-ray-induced double-strand breaks.**

## INTRODUCTION

*Saccharomyces cerevisiae RAD52* was initially isolated in a genetic screen for mutants that were sensitive to radiation and to agents known to cause DNA double-strand breaks (DSBs) (1,2). Further analysis showed that *rad52* mutant strains display a pleiotropic phenotype, including defects in DNA DSB repair, reduced mitotic and meiotic recombination rates, deficient mating-type switching, elevated mutation rates, increased chromosome loss and low spore viability (3–8). The importance of *RAD52* is underscored by its conservation through evolution in species ranging from yeast to humans (9–14).

Although the sequence of *S.cerevisiae RAD52* has been known for more than 20 years (15), the precise gene product(s) have not been defined. This is due to the presence of five potential translation start sites in the *RAD52* open reading frame (ORF). Previously, analysis by S1 nuclease digestion of the *RAD52*-encoded mRNA has shown that a major transcript starts 10 nt downstream of the second ATG triplet in the ORF (15). In accordance with this, most biochemical analyses of Rad52 have employed protein expressed from the third AUG triplet, leaving open the possibility that important aspects of the protein have been overlooked. It is possible that endogenous expression of Rad52 is more complex, as has been shown for other genes with multiple start codons. For example, the *SUC2* invertase gene in yeast contains multiple ATG codons, and initiation at the first start site yields a glycosylated, secreted invertase protein. However, when translation initiates from a downstream AUG, the result is an unglycosylated invertase protein that remains in the cell (16).

The ribosomal 'scanning' model (17–20) proposes a mechanism by which eukaryotic ribosomes select the translation initiation site. Briefly, the 40S ribosomal subunit binds near the free 5′ end of an mRNA and migrates through the noncoding region scanning for a translational start site. In yeast and higher eukaryotes, 95% of translation initiates at the AUG triplet near the 5′ end (21,22). However, some eukaryotic transcripts have more complex arrangements and the sequence surrounding the AUG codon can either enhance or inhibit initiation of translation at that site. Hence, if the first AUG triplet encountered occurs in a suboptimal

sequence recognition context, some 40S subunits will bypass this triplet and initiate translation at a downstream start site by a process termed 'leaky scanning' (23–27).

Three features near the start codon influence leaky scanning. First, multiple studies have analyzed mRNA sequences and the context surrounding the AUG triplet in many yeast genes to determine whether a consensus sequence exists (22,28,29). From these studies, only the preference for a purine at position −3 is consistent. This preference has been confirmed by mutational analysis of the 5′ upstream region of the *CYC7* gene fused to the coding region of *lacZ* (27). In that study, the preferred nucleotide at position −3 was A>G>C>T, with relative protein translational levels 100:94:69:54 (27). In the case of the *S.cerevisiae RAD52* gene, the nucleotide at the −3 position for the five ATG codons (from 5′ to 3′) is C, C, T, A and G, respectively.

Second, the length of the 5′ mRNA leader sequence also influences leaky scanning (30,31). In yeast, the majority of leader sequences (70%) range from 20 to 60 nt, which is sufficiently long to support initiation of translation (22). Inspection of the *RAD52*-encoded mRNA by S1 nuclease digestion (15) shows that a major transcript starts 10 nt downstream of the second ATG triplet, thus allowing for a minimum leader sequence of 47 nt upstream of the remaining ATGs.

Finally, experimental data from mammalian systems suggest that a stable stem–loop structure 12–15 nt downstream of a start codon can cause the scanning ribosome to pause with its AUG-recognition center right over the initiator codon, providing more time for the recognition of this start site (32). In the *S.cerevisiae RAD52*-encoded mRNA, a potential stem–loop structure is located downstream of the fifth start codon. This hairpin may influence the preference of the ribosome for the start codons differently as the distance separating the stem–loop structure from the third, fourth and fifth start codons is 33, 21 and 15 nt, respectively.

Size determination of the Rad52 protein by gel-electrophoresis followed by immunoblot analysis typically detects multiple protein species. The existence of different Rad52 species suggests a promiscuous start codon choice. In addition, some of the multiple protein species could also result from post-translational modification and/or degradation. Here we show that yeast *RAD52*-encoded mRNA produces Rad52 expressed from three different start sites and that DNA DSB repair is supported by the three protein species. In addition, Rad52 is phosphorylated both in a cell cycle-independent and cell cycle-dependent manner and these modifications require the presence of the Rad52 C terminus. Finally, maintenance of wild-type Rad52 protein levels is important for efficient repair of some types of DNA damage.

## MATERIALS AND METHODS

### Genetic methods, yeast strains, site-directed mutagenesis and plasmids

Media were prepared as described previously and contains twice the amount of leucine (60 mg/l) and the yeast strains were manipulated using standard genetic techniques (33). All strains used in this study are *RAD5* derivatives of

**Table 1.** List of strains

| Strain[a] | Genotype |
|---|---|
| W1588-4C[b] | *MAT**a** ade2-1 can1-100 his3-11,15 leu2-3,112 trp1-1 ura3-1* |
| J795 | *MAT**a** rad52-E24Stop* |
| J789 | *MAT**a** rad52-M34A* |
| J792 | *MAT**a** rad52-FS3-4* |
| J794 | *MAT**a** rad52-E36Stop* |
| J790 | *MAT**a** rad52-M38A* |
| J793 | *MAT**a** rad52-FS4-5* |
| J791 | *MAT**a** rad52-M40A* |
| J1100 | *MAT**a** rad52-E24StopM38AM40A* |
| J1104 | *MAT**a** rad52-E24StopM34AM38A* |
| W2263-14B | *MAT**a** rad52::HIS5* |
| W4023-4D | *MAT**a** rad52::HIS5* |
| J883 | *MAT**a** rad52-327Δ* |
| W3801-2D | *MAT**a** leu2-ΔBstEII lys2ΔTRP1 rad52-Y66**o** SUP4-**o*** |
| W2846 | *MAT**a** leu2-ΔBstEII lys2ΔTRP1* |
| | *MATα leu2-ΔEcoRI LYS2 trp1-1* |
| W2847 | *MAT**a** leu2-ΔBstEII lys2ΔTRP1 rad52-E24Stop* |
| | *MATα leu2-ΔEcoRI LYS2 trp1-1 rad52-E24Stop* |
| W2848 | *MAT**a** leu2-ΔBstEII lys2ΔTRP1 rad52-M34A* |
| | *MATα leu2-ΔEcoRI LYS2 trp1-1 rad52-M34A* |
| W2849 | *MAT**a** leu2-ΔBstEII lys2ΔTRP1 rad52-FS3-4* |
| | *MATα leu2-ΔEcoRI LYS2 trp1-1 rad52-FS3-4* |
| W2850 | *MAT**a** leu2-ΔBstEII lys2ΔTRP1 rad52-E36Stop* |
| | *MATα leu2-ΔEcoRI LYS2 trp1-1 rad52-E36Stop* |
| W2851 | *MAT**a** leu2-ΔBstEII lys2ΔTRP1 rad52-M38A* |
| | *MATα leu2-ΔEcoRI LYS2 trp1-1 rad52-M38A* |
| W2852 | *MAT**a** leu2-ΔBstEII lys2ΔTRP1 rad52-FS4-5* |
| | *MATα leu2-ΔEcoRI LYS2 trp1-1 rad52-FS4-5* |
| W2853 | *MAT**a** leu2-ΔBstEII lys2ΔTRP1 rad52-M40A* |
| | *MATα leu2-ΔEcoRI LYS2 trp1-1 rad52-M40A* |
| W2854 | *MAT**a** leu2-ΔBstEII lys2ΔTRP1 rad52::HIS5* |
| | *MATα leu2-ΔEcoRI LYS2 trp1-1 rad52::HIS5* |
| W3765 | *MAT**a** leu2-ΔBstEII lys2ΔTRP1 rad52-E24StopM38AM40A* |
| | *MATα leu2-ΔEcoRI LYS2 trp1-1 rad52-E24StopM38AM40A* |
| W3766 | *MAT**a** leu2-ΔBstEII lys2ΔTRP1 rad52-E24StopM34AM38A* |
| | *MATα leu2-ΔEcoRI LYS2 trp1-1 rad52-E24StopM34AM38A* |
| W6257 | *MAT**a** leu2-ΔBstEII lys2ΔTRP1 rad52-Y66**o** SUP4-**o*** |
| | *MATα leu2-ΔEcoRI LYS2 trp1-1 rad52-Y66**o** SUP4-**o*** |
| UM21-11D[c] | *MAT**a** rad52-409-412Δ* |

[a]All strains used in the study are *RAD5+* derivatives of W303 (34).
[b]Zou and Rothstein 1997 (35).
[c]Mortensen laboratory collection.

W303 and are listed in Table 1 (34,35). The sequences of the oligonucleotides used to introduce the specific mutations in *RAD52* are listed in Table 2.

The pRS414-*RAD52 CEN* vectors containing single start codon mutants were made by site-directed mutagenesis, as described previously (36). The *rad52* point mutations were integrated into the *RAD52* genomic locus using a cloning-free PCR-based allele replacement method (37). Individual *rad52* point mutations were PCR amplified from the corresponding pRS414-*RAD52 CEN* vector in 100 µl reactions. For both triple *rad52* mutant strains (*E24Stop M38A M40A* and *E24Stop M34A M38A*), the changes were introduced by three sets of PCRs. The first PCR generates overlapping fragments containing different mutations. In the second PCR, the two overlapping fragments were fused. Fragments containing the N-terminal and C-terminal two-thirds of the *Kluyveromyces lactis URA3* gene were amplified. The final PCR fuses the *K.lactis URA3* fragments to the *RAD52* fragments. The products were gel purified and co-transformed into wild-type yeast strain W1588-4C to create the single *rad52* mutants

**Table 2.** List of oligonucleotide primers to make mutants

| Primer | Sequence |
| --- | --- |
| Adapt-a | 5′-CATGGTGGTCAGCTGGAATTCGATGATGTAGTTTCTGGTT |
| Adapt-b | 5′-CATGGCAATTCCCGGGGATCGTGATTCTGGGTAGAAGATCG |
| ARad52 | 5′-AATTCCAGCTGACCACCATGCAACTCCCTTGGCGTCTG |
| BRad52 | 5′-GATCCCCGGGAATTGCCATGGAGCATTACCAAACCCTCTC |
| 3′-int | 5′-GAGCAATGAACCCAATAACGAAATC |
| 5′-int | 5′-CTTGACGTTCGTTCGACTGATGAGC |
| AdapB-M40AM38A | 5′-CCCCGGGAATTGCCATGCCGAAAACGGGCTTCTTCTCATCCGCATCCGCGAT |
| M38AM40A | 5′-GATGAATGAAATCGCGGATGCGGATGAGAAGAAGC |
| M38AM34A | 5′-GGGCTTCTTCTCATCCATATCCGCGATTTCATTGGCCAACAACAC |
| M34AM38A | 5′-GTGTTGTTGGCCAATGAAATCGCGGATATGGATGAG |
| A-4Ala | 5′-AATTCCAGCTGACCACCATGCGCTAAGCAGGCACCAGCTGC |
| Bwd2Ala | 5′-GCGGCAACAAACGCGATTTGTTCTGCC |
| Fwd2Ala | 5′-GGCAGAACAAATCGCGTTTGTTGCCGC |
| R52Bwd2353-B | 5′-GATCCCCGGGAATTGCCATGCCTTAGAAGGCGGCGCAAACCG |
| AR52-1769 | 5′-AATTCCAGCTGACCACCATGCCCTGCTGAGGCTAACAGTAAAAACAGCAG |
| 4AlaBwd | 5′-GCCTCTGGGTTTGCAGCCGCAGCTGGTGCCTGCTTAGC |
| M34A | 5′-GGTGTGTTGTTGGCCAATGAAATTATGGATATGG |
| M38A | 5′-TGTTGTTGATGAATGAAATCGCGGATATGGATGAGAAG |
| M40A | 5′-GTTGATGAATGAAATTATGGATGCGGATGAGAAGAAGCCCG |
| E24Stop | 5′-GCCAAGAACTGCTTAAGGTTCTGGTGGC |
| E36Stop | 5′-GGTGTGTTGTTGATGAATTAAATTATGGATATGG |
| FS3-4 | 5′-GGTGTGTTGTTGATGAATGCCAAATTATGGATATGG |
| FS4-5 | 5′-GTTGATGAATGAAATTATGGAGGTATGGATGAGAAG |
| Y66o | 5′-GGACAAGAAATTAGGACCTGAATAAATCTCCAAGAGAG |

The first six oligonucleotide primers were described previously (36,37).

or into J795 (*E24Stop*) to create the triple *rad52* mutations. Transformants were selected on SC-Ura and 'pop-out' recombinants that excised the *K.lactis URA3* marker were selected on SC-5-fluoro-orotic acid medium. All *rad52* point mutations were designed to generate a restriction nuclease polymorphism and were further confirmed by DNA sequencing.

pRS423-*RAD52*, a 2μ vector based on pRS423 (38) carrying the entire *RAD52*-containing SalI fragment (15) was used to make the pRS423-*M34A* plasmid. Briefly, pRS423-*RAD52* was linearized with restriction enzyme AgeI and transformed into the J789 yeast strain to gap-repair the chromosomal *rad52-M34A* mutation onto the plasmid. The *rad52* point mutation alters a restriction enzyme site and was confirmed by PCR and restriction enzyme analysis.

### Analysis of sensitivity to gamma-irradiation

The sensitivity to gamma rays was analyzed as described previously (39) and quantitative survival curves were made by calculating ln(percent survival) for each dose. The slope (α) of the resulting straight line can be used to calculate an $LD_{37}$ value $[-\ln(1/0.37)/\ln(\alpha)]$. The $LD_{37}$ value represents the dose in krad necessary to induce a mean of one lethal hit per cell and was used to quantitatively compare survival of different strains.

The effect of overexpressing the *M34A* mutant for gamma-irradiation survival was determined as follows. An *M34A* strain (J789) was transformed with 2μ pRS423 (empty vector control), pRS423-*RAD52* and pRS423-*M34A*. Wild-type (W1588-4C) was transformed with pRS423 as a control. Overnight cultures were plated on SC-His medium and survival after gamma-irradiation was measured.

### Spontaneous *LEU2* heteroallelic recombination

Mitotic interchromosomal recombination between the *leu2-ΔEco*RI and *leu2Δ-Bst*EII heteroalleles was measured in diploid strains as described previously (39), except that the strains were pre-grown in liquid SC medium before plating. Plating efficiency and the number of recombinants were determined by plating an appropriate number of cells on SC and SC-Leu plates, respectively. For each strain, 5–9 independent trials were carried out and the corresponding recombination rates and their standard deviations were calculated according to the method of the median described previously (40).

### Cell cycle synchronization, protein extraction and immunoblot analysis

Yeast cultures were grown at 30°C to early/mid-log phase in YPD (pH 3.7). Cells were arrested in $G_1$ phase by incubating in the presence of α-mating factor for 90 min (3.4 μg/ml; Sigma, St Louis, MO). Next, cells were released from the $G_1$-arrest by washing in 1 vol four times and resuspending the cells in 1 vol of pre-warmed YPD (pH 5.6). An aliquot of 1.5 ml samples were taken at different time points after release from $G_1$. For protein samples from unsynchronized cells, the cultures were grown at 30°C to early/mid-log phase in YPD before aliquots were taken. The cells were harvested by centrifugation and resuspended in 0.5 ml of 25% TCA. After centrifugation, the resulting pellets were washed twice with 90% acetone, resuspended in 1% SDS and an equal volume of glass beads added. The samples were vortexed 3 times for 30 s and incubated on ice for 1 min between each round of vortexing. An equal volume of loading buffer [60 mM Tris–HCl, pH 6.8, 25% glycerol, 2% SDS, 14.4 mM 2-mercaptoethanol, 0.1% bromophenol

blue and 2× proteinase protease inhibitor (catalog no. 1697498; Boehringer, Mannheim, Germany)] was added and the samples were boiled for 5 min before loading. Rad52 protein species were separated by SDS–PAGE (10% polyacrylamide, polyacrylamide/bis 37.5:1, 20 cm × 16 cm × 1 mm gels) and immunoblot analysis performed as described previously (41).

### Fluorescence-activated cell sorting

Fluorescence-activated cell sorting (FACS) analysis was performed to determine DNA content of cells collected from cell cycle synchronization experiments. At each time point, a 1 ml sample was collected and fixed in 70% ethanol overnight at room temperature. Ethanol was removed and the cells were washed once with 50 mM sodium citrate. The pellet was resuspended in 50 mM sodium citrate and 0.25 mg/ml RNase A and incubated at $50°C$ for 1 h. Proteinase K was added to a final concentration of 1 mg/ml and incubated at $50°C$ for 1 h. An equal volume of 50 mM sodium citrate containing 8 $\mu$g/ml propidium iodide was added and the samples placed on a shaker in the dark at room temperature for 30 min. Samples were sonicated and then analyzed using a FACS Calibur (Becton Dickinson, Franklin Lakes, NJ).

### Phosphatase treatment

Rad52 protein was isolated as described above, except that, after the acetone washes, the pellet was resuspended in NP-40 buffer (50 mM Tris–HCl, pH 8.0, 1% NP-40 and 150 mM NaCl). Immediately, before use, this buffer was supplemented with complete mini EDTA-free protease inhibitor cocktail (Roche, catalog no. 1183617000). An equal volume of glass beads was added and the samples were vortexed 3 times for 30 s and incubated on ice for 1 min in between each vortexing. The samples were treated with $\lambda$-phosphatase (New England Biolabs) for 45 min at $30°C$, an equal volume of loading buffer was added and they were boiled for 5 min before loading. Rad52 protein species were separated by SDS–PAGE and immunoblot analysis performed as described previously (41).

### Preparation of Rad52 extracts from *E.coli*

*E.coli* strain M15(pREP4) was transformed with pQE60-Rad52-His$_6$ (42) and plated on Luria–Bertani broth containing 100 $\mu$g/ml ampicillin and 25 $\mu$g/ml kanamycin. An overnight culture was grown at $37°C$, diluted 1:40 and

grown for an additional 3 h. At this point, the expression of Rad52-HIS$_6$ was induced by adding IPTG to a final concentration of 1 mM. After a 1 h induction, the cells were pelleted by centrifugation and the pellet was resuspended in 5 ml equilibration buffer (20 mM phosphate buffer, pH 8.0, 400 mM NaCl, 10% glycerol, 1 mM PMSF, 0.66 ml/ml lysozyme and 5% Triton X-100). The sample was sonicated (Ultrasonic W-385 Processor, Heat System-Ultrasonics, Inc.) five times for 1 min separated by a 2 min ice incubation and subsequently spun for 5 min at 18 000 r.c.f. Rad52-HIS$_6$ protein was separated by SDS–PAGE and immunoblot analysis was performed as described above.

### Statistical analysis

A *t*-test was used to determine the significance for gamma-ray survival differences.

## RESULTS

### The first two potential start codons in *RAD52* are not used

Analysis of wild-type *S.cerevisiae* Rad52 reveals multiple protein species with different electrophoretic mobilities (42–45). In the resolution obtained in the present study, 3–4 Rad52 protein bands were typically detected for the wild-type strain. The apparent molecular weight of the three Rad52 protein bands in Figure 1A are $\sim$54, 57 and 60 kDa. The different Rad52 species may represent the result of differential start codon usage and/or post-translational modifications. To investigate these possibilities, *RAD52* sequences obtained from three other species from the *Saccharomyces sensu stricto* group (*S.paradoxus*, *S.uvarum* and *S.monacensis* var. *pastorianus*) were inspected for the presence of multiple potential start codons. As shown in Figure 1B, the first, third, fourth and fifth *S.cerevisiae* ATG codons are present in the other three *Saccharomyces* species. However, in the three closely related species, the first start codon is not in-frame with the remaining *RAD52* ORFs due to single base-pair deletions and insertions within the first 70 nt. Furthermore, stop codons following the first ATG start site prevent the formation of a peptide of significant length in all three related species. Hence, in *S.paradoxus*, *S.uvarum* and *S.monacensis* Rad52 protein can only be translated from the ATGs that are equivalent to the third, fourth and fifth start
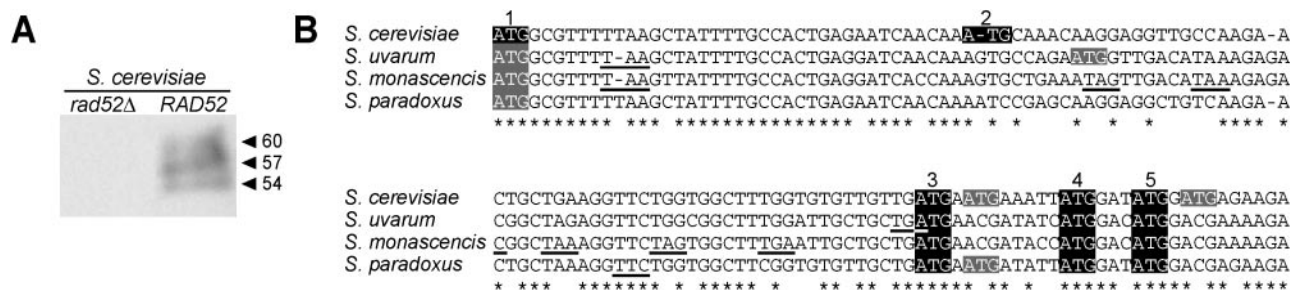


**Figure 1.** Analysis of Rad52 protein. (**A**) Immunoblot of *rad52Δ* and *RAD52* using anti-Rad52 antibody. Approximate molecular weights (kDa) corresponding to the observed mobility are indicated. (**B**) Alignment of the *RAD52* sequence from four species that belong to the *Saccharomyces sensu stricto* group: *S.cerevisiae*, *S.paradoxus*, *S.uvarum* and *S.monacensis* . ATG codons in-frame with the third ATG codon in *S.cerevisiae*. ATG codons out-of-frame with the third ATG codon in *S.cerevisiae*. Stop codons in-frame with the previous ATG encountered are underlined. * denotes conserved nucleotides.

**Figure 2.** Analysis of the third start codon. Note, *RAD52*-mRNA initiates 10 nt downstream of start codon 2 (15). (**A**) Schematic diagram of *M34A*, *E36Stop* and *FS3-4* mutant strains. *M34A* results from a methionine-to-alanine substitution at amino acid 34. *E36Stop* results from a stop codon inserted at amino acid 36. *FS3-4* mutant results from a frameshift mutation inserted between the third and fourth ATGs. In *FS3-4*, translation initiated upstream of the fourth start codon results in truncation at amino acid 63. Hence in these mutant strains, Rad52 can only be expressed from the fourth and/or fifth start codons. (**B**) Schematic diagram of *E24Stop M38A M40A* mutant having a stop codon at residue 24, and two methionine-to-alanine substitutions at amino acids 38 and 40. In this mutant, translation can only start at the third start codon. M, methionine residues indicating the position of the ATG codons. A, alanine residues substitute the methionine amino acids at the indicated positions. Residues in gray are not productive for translation start. (**C**) Survival curves of haploid strains after increasing doses of gamma-ray-induced DNA damage. Black diamond, *RAD52*; open circle, *rad52* null; black circle, *M34A*; black square, *FS3-4*; inverted open triangle, *E36Stop*; and open diamond, *E24Stop M38A M40A*. (**D**) Gamma-ray survival after overexpression of the *RAD52* and *M34A* genes from 2μ plasmids. Cells carrying 2μ plasmids were grown and plated on SC-His medium. Open square, *RAD52* transformed with pRS423 (empty vector); open triangle, *M34A* transformed with pRS423-*M34A*; inverted black triangle, *M34A* transformed with pRS423; and black triangle, *M34A* transformed with pRS423-*RAD52*.

codons in *S.cerevisiae*. These results suggest that Rad52 translation in *S.cerevisiae* starts from the third, fourth and/or fifth start codons. To test this hypothesis, the glutamic acid codon at position 24 (between the second and third potential ATGs) was replaced with a stop codon. As expected, this mutant strain is as resistant to gamma-irradiation as the wild-type strain, and immunoblot analysis demonstrated that the mutation did not significantly change the Rad52 protein level (data not shown). In addition, the analysis detects multiple protein species with the same electrophoretic mobilities as those observed for wild-type Rad52 (data not shown).

### Rad52 protein contribution from the third start codon

To test the possibility that the multiple Rad52 species detected by protein-blot analysis result from differential usage of the third, fourth and fifth start codon, various point mutations were created to analyze the contribution from the third start codon. First, three different types of mutations: a methionine-to-alanine substitution at amino acid 34 (*M34A*), a stop codon (*E36Stop*) and a frameshift mutation (*FS3-4*) were individually introduced to disrupt translation from the third start codon (Figure 2A). Strains that contain either of the two latter mutations produce short peptides (a 2 amino acid peptide and 28 amino acid frameshifted peptide, respectively) if translation is attempted from the third start codon. Hence, in these three mutant strains, Rad52 protein can only be expressed from the fourth and/or fifth start codons. To determine the sensitivity of these mutants to gamma-irradiation, survival curves were determined and $LD_{37}$ values were calculated (see Materials and Methods). Comparison of the resulting $LD_{37}$ values demonstrates that each mutant strain is ∼3-fold more sensitive to gamma-irradiation than the wild-type strain (Figure 2C and Table 3). In contrast, a *rad52* null (*rad52Δ*) strain is 20-fold more sensitive than the wild-type strain.

Second, to analyze whether expression from the third start codon is sufficient to repair DNA damage, a triple mutant strain, *E24Stop M38A M40A*, was made. This

**Table 3.** The effect of start codon mutants on gamma-ray sensitivity (LD$_{37}$) and mitotic heteroallelic recombination rate

| Strain | Gamma-ray sensitivity (LD$_{37}$)[a] | Mitotic recombination rate $\times 10^{-6b}$ |
|---|---|---|
| *RAD52* | 51.2 ± 2.9 | 1.2 ± 0.2 |
| *E24Stop* | 56.5 ± 3.6 | 1.7 ± 0.3 |
| *M38A* | 52.8 ± 5.7 | 1.1 ± 0.2 |
| *M40A* | 44.2 ± 1.6 | 0.5 ± 0.1 |
| *E24Stop M34A M38A* | 53.8 ± 8.9 | 1.0 ± 0.2 |
| *M34A* | 19.1 ± 1.0 | 0.4 ± 0.1 |
| *FS3-4* | 15.8 ± 0.1 | 0.8 ± 0.1 |
| *E36Stop* | 16.9 ± 0.4 | 2.0 ± 0.3 |
| *E24Stop M38A M40A* | 14.8 ± 0.1 | 0.6 ± 0.1 |
| *FS4-5* | 6.2 ± 0.1 | 0.2 ± 0.03 |
| *rad52::HIS5* | 2.6 ± 0.1 | 0.006 ± 0.003 |
| *Y66o SUP4-o* | 21.0 ± 1.7 | 0.3 ± 0.04 |

[a]LD$_{37}$, the dose in krad necessary to induce a mean of one lethal hit per cell, as described in Materials and Methods.
[b]Recombination rate (events per cell per generation) is presented as the mean ± SD as described in Materials and Methods.

mutant strain has a stop codon at amino acid 24 and two methionine-to-alanine changes at amino acids 38 and 40; thus, Rad52 can only be produced from the third start codon, M34 (Figure 2B). The survival curves and LD$_{37}$ values indicate that this strain is ~3-fold more sensitive to gamma-irradiation than the wild-type strain (Figure 2C and Table 3). In summary, translation from the third start codon is necessary, but not sufficient for full Rad52 activity (Figure 2C).

The slightly increased gamma-ray sensitivity of the *M34A*, *E36Stop*, *FS3-4* and *E24Stop M38A M40A* mutant strains may indicate that a combination of the different Rad52 protein species expressed from the third, fourth and fifth start codons are required for full DNA repair activity. Alternatively, the phenotype of these mutant strains may result from variations in Rad52 protein levels. To distinguish between these possibilities, the *RAD52* and *M34A* alleles were overexpressed from 2μ plasmids (pRS423-*RAD52* and pRS423-*M34A*, respectively) and survival curves after gamma-irradiation determined (Figure 2D). Overexpression of *M34A* or wild-type Rad52 in the *M34A* background results in gamma-ray survival curves that are not statistically different. The survival of these two strains is also not significantly different from a wild-type strain transformed with an empty vector (pRS423). However, these three strains are more resistant to gamma-irradiation than *M34A* itself transformed with the empty vector. Thus, the suppression of the gamma-ray sensitivity of *M34A* by its overexpression shows that the phenotype of *M34A* expressed from its endogenous promoter is likely due to reduced protein levels (see below).

**Rad52 protein contribution from the fourth and fifth start codons**

To determine the role of the fourth and fifth start codons, methionine-to-alanine substitutions were individually introduced into the cell (*M38A* and *M40A*, respectively) to prevent translation initiation from these two start codons (Figure 3A). None of these start codons is essential since both strains are

as gamma-ray resistant as the wild-type strain (Figure 3B and Table 3).

Next, we constructed *FS4-5* to obtain an independent estimate of the amount of protein initiated from start codon five in wild-type cells (Figure 3C). The frameshift mutation results in a dramatic increase in gamma-ray sensitivity, which could be due to either decreased Rad52 protein levels or a repair defect of this shorter protein (Figure 3D and Table 3; Figure 4, lane 8). To distinguish between these possibilities, a triple mutant was created that has a stop codon at amino acid 24 and two methionine-to-alanine codon changes at codons 34 and 38 (*E24Stop M34A M38A*) (Figure 3C). We find that the increased expression of Rad52 from the fifth start codon in this construct provides wild-type levels of Rad52 activity (Figure 3D and Table 3; Figure 4, lane 10). Taken together, these results indicate that the fifth start codon normally contributes a minor amount of Rad52 protein, which is, however, fully functional for DSB repair after gamma-irradiation.
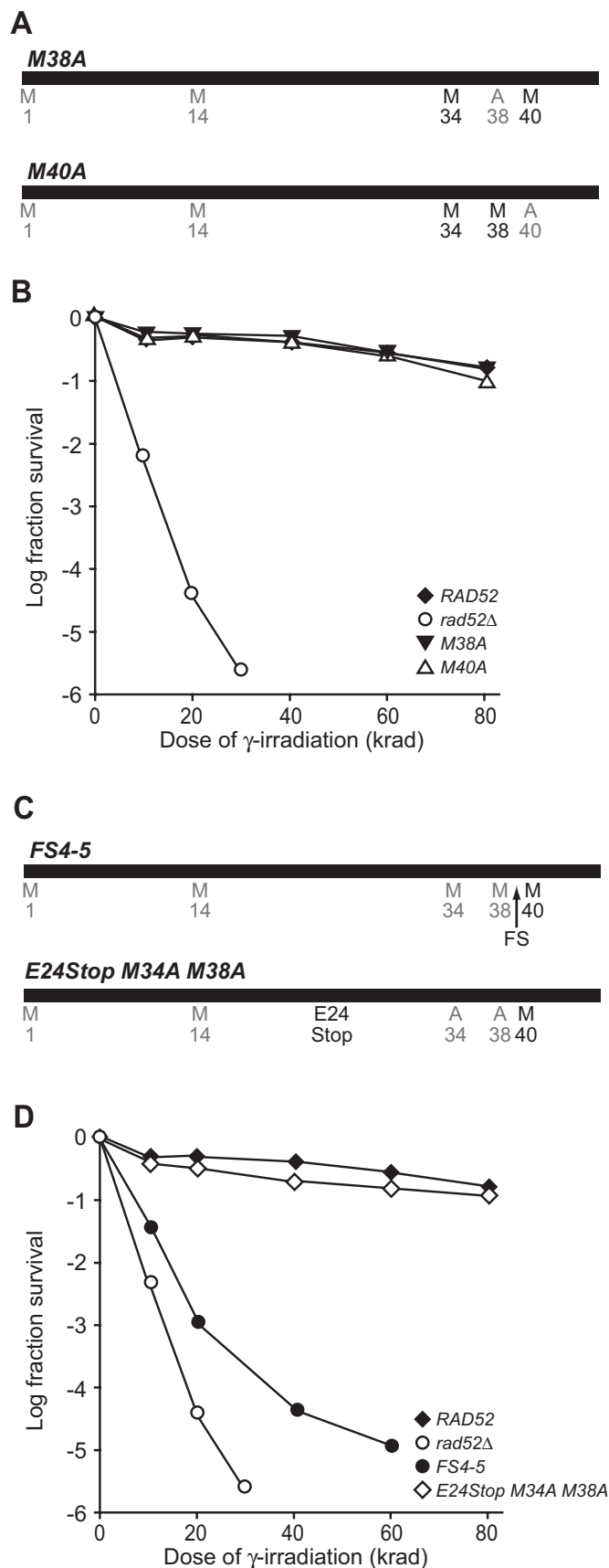
The increased gamma-ray sensitivity of *FS4-5* compared to *E24Stop M34A M38A* suggests that Rad52 protein levels are important for efficient repair of DSBs (Figure 3D and Figure 4, lanes 8 and 10). To address this issue, a strain was made that expresses decreased levels of wild-type Rad52 protein by combining a *SUP4-o* nonsense suppressor with a *RAD52* ORF containing an ochre termination codon (*Y66o*). Since ochre suppression is not complete (46,47), this strain expresses Rad52 at 25% of wild-type levels as determined by quantitative immunoblot analysis (data not shown). At this reduced protein level, we find that the resulting LD$_{37}$ value is 2- to 3-fold lower than that of wild-type (Table 3), demonstrating that Rad52 becomes limiting for gamma-ray survival at reduced protein levels.

**Spontaneous heteroallelic recombination is reduced in strains with decreased levels of Rad52**

To investigate the possibility that distinct Rad52 species influence Rad52 functions differentially, spontaneous interchromosomal heteroallelic recombination was measured between two non-functional *leu2* heteroalleles, *leu2Δ-Bst*EII and *leu2Δ-Eco*RI (39) for all the *rad52* mutants presented in this study. Using this assay, mitotic recombination was investigated in diploid cells homozygous for the *RAD52* alleles presented above (Table 3). Compared to a wild-type strain, a *rad52Δ* strain has a 200-fold lower recombination rate. Among the different start codon mutants, *FS4-5* shows the greatest decrease in the rate of spontaneous recombination, consistent with it having decreased protein levels and being the most sensitive to ionizing radiation. In addition, there is a 4-fold reduction in the rate of spontaneous recombination in *Y66o SUP4-o* strains compared to wild-type cells (Table 3). Thus, at reduced levels, Rad52 protein becomes limiting for spontaneous heteroallelic recombination.

**Rad52 is phosphorylated in a cell cycle-independent and cell cycle-dependent manner**

Some of the multiple Rad52 protein bands observed for the wild-type strain are accounted for by the promiscuous choice of start codons. For example, the 54 kDa protein band jointly represents Rad52 translated from the fourth and fifth start

**A**

**M38A**

| M | M | M | A | M |
|---|---|---|---|---|
| 1 | 14 | 34 | 38 | 40 |

**M40A**

| M | M | M | M | A |
|---|---|---|---|---|
| 1 | 14 | 34 | 38 | 40 |

**B**

**C**

**FS4-5**

| M | M | M | M | M |
|---|---|---|---|---|
| 1 | 14 | 34 | 38 | 40 |

FS

**E24Stop M34A M38A**

| M | M | E24 | A | A | M |
|---|---|---|---|---|---|
| 1 | 14 | Stop | 34 | 38 | 40 |

**D**

codons since it is not detected in *E24Stop M38A M40A*, which can only produce protein from the third start codon (Figure 4, lane 9). This is further supported by the observation that the 54 kDa band is present in both *M38A* and *M40A* where the fourth and fifth start codons are removed individually (Figure 4, lanes 5 and 6). In addition, mutant strains *E36Stop*, *M34A* and *FS3-4* (Figure 4, lanes 3, 4 and 7), which can express Rad52 protein only from the fourth and fifth start codons, produce a 57 kDa band in addition to the expected 54 kDa band. The presence of the 57 kDa bands suggests that these Rad52 species are post-translationally modified. Furthermore, multiple bands are produced in mutants where Rad52 translation can only initiate from a single start codon (*FS4-5*, *E24Stop M38A M40A* and *E24Stop M34A M38A*) (Figure 4, lanes 8–10). To unequivocally determine the mobility of unmodified protein, the yeast *RAD52* gene was expressed in *E.coli* from the third start codon to compare its migration pattern to that of wild-type yeast protein. Rad52 expressed in *E.coli* produces a single band that co-migrates with the 57 kDa protein band present in yeast extracts of wild-type cells (Figure 5A). $G_1$-arrested yeast cells expressing Rad52 only from the third start site (*E24Stop M38A M40A*) produce 57 and 60 kDa bands (Figure 5B, 0 min). When these cells are released into S phase, an additional band appears (63 kDa) (Figure 5B, 45 min), similar to what we previously showed for wild-type Rad52 (43). Together these observations show that post-translational modification is responsible for several of the Rad52 species observed.

To determine whether the post-translational modification is phosphorylation, protein extracts from $G_1$-arrested wild-type cells were treated with λ-phosphatase. The multiple Rad52 species collapse into two distinct protein bands that co-migrate with the 54 and 57 kDa protein bands from untreated wild-type cells (Figure 5C, 0 min). The 63 kDa cell cycle specific band also disappears after λ-phosphatase treatment (Figure 5C, 60 min). Finally, λ-phosphatase treatment of protein extracts from *E24Stop M38A M40A*, which can only produce Rad52 protein from the third start codon, merges the different protein species into a single 57 kDa Rad52 band (data not shown). Rad52 dephosphorylation also occurs after treatment with protein phosphatase 1, which is specific towards phosphoserines and phosphothreonines, but not after T-cell protein tyrosine phosphatase treatment, a phosphotyrosine specific phosphatase (data not

**Figure 3.** Mutational analysis of the fourth and fifth start codons. (**A**) Schematic diagram of *M38A* and *M40A* mutants. *M38A* or *M40A* mutant strains result from methionine-to-alanine substitutions at amino acid 38 or 40, respectively. Residues in gray are not productive for translation start. (**B**) Survival curves of haploid strains after exposure to gamma-irradiation. Black diamond, *RAD52*; open circle, *rad52* null; inverted black triangle, *M38A*; open triangle, *M40A*. (**C**) Schematic diagram of *E24Stop M34A M38A* and *FS4-5* mutants. The *E24Stop M34A M38A* mutant strain has a stop codon at residue 24 and two methionine-to-alanine substitutions at amino acids 34 and 38. In this triple mutant, translation can only start at the fifth start codon. The *FS4-5* mutant results from a frameshift mutation inserted between the fourth and fifth ATGs. In *FS4-5*, translation initiated upstream of the fifth start codon results in truncation at amino acid 63. M, methionine residues indicating the position of the ATG codons. A, alanine residues substitute the methionine amino acids at the indicated positions. Residues in gray are not productive for translation start. (**D**) Survival curves of haploid strains after exposure to gamma-irradiation. Black diamond, *RAD52*; open circle, *rad52* null; black circle, *FS4-5*; and open diamond, *E24Stop M34A M38A*.
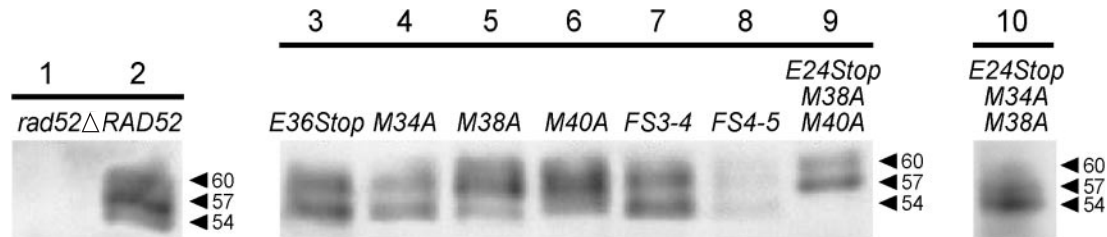
**Figure 4.** Protein analysis of the *rad52* mutants that disrupt the third, fourth and fifth start codons. Rad52 was examined by immunoblot analysis using an anti-Rad52 antibody. Lane 1, *rad52* null; lane 2, *RAD52*; lane 3, *E36Stop*; lane 4, *M34A*; lane 5, *M38A*; lane 6, *M40A*; lane 7, *FS3-4*; lane 8, *FS4-5*; lane 9, *E24Stop M38A M40A*; and lane 10, *E24Stop M34A M38A*. Equal amounts of total protein were loaded in each lane on the gel. Approximate molecular weights (kDa) corresponding to the observed mobility are indicated.
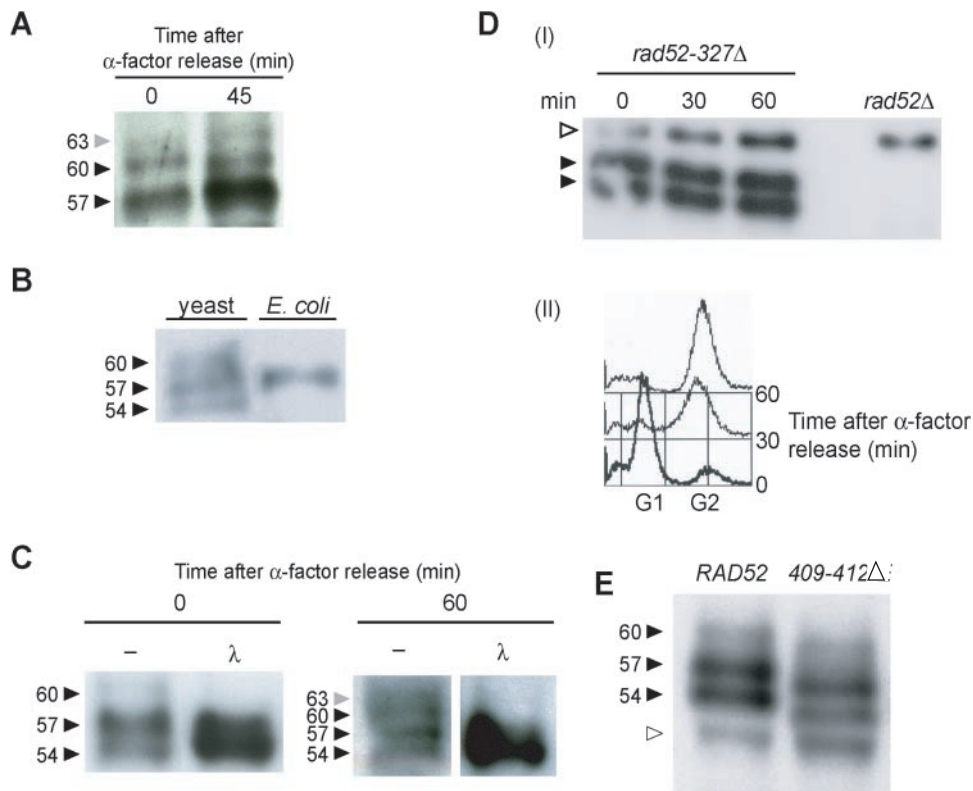


**Figure 5.** Phosphorylation of Rad52. (**A**) Immunoblot using anti-Rad52 antibody of *RAD52* expressed in yeast and *E.coli* cells. (A–E) Black arrowheads: Rad52 protein bands of different electrophoretic mobilities. (B and C) Gray arrowhead: cell cycle-dependent phosphorylation of Rad52. (**B**) Cell cycle-independent and cell cycle-dependent phosphorylation of Rad52 protein in *E24Stop M38A M40A*. Cells were synchronized in $G_1$ by α-factor and released into S phase at time zero. Protein extracts were made from arrested cells (time zero) and at 45 min following α-factor release. (**C**) Dephosphorylation of Rad52. Wild-type *RAD52* cells were synchronized in $G_1$ by α-factor and released into S phase at time zero. Protein extracts were made from arrested cells (time zero) and at 60 min following α-factor release. λ, indicates that protein extracts were treated with λ-phosphatase; −, indicates no phosphatase treatment. (**D**) Immunoblot analysis of cell cycle synchronized *rad52-327*delta cells. Protein extracts were made 0, 30 and 60 min after release from $G_1$-arrested cells. Rad52 was examined by immunoblot analysis using anti-Rad52 antibody (I). Samples were subjected to FACS analysis to determine DNA content of cells at each time point (II). (D and E) Empty arrowhead: a protein band non-specifically recognized by the anti-Rad52 antibody also present in the *rad52* null. (**E**) Immunoblot of *RAD52* and *rad52-409-412*delta strains.

shown). In summary, these results demonstrate that Rad52 is phosphorylated at serine and/or threonine residues in both a cell cycle-independent and cell cycle-dependent manner.

### Post-translational modification of Rad52 requires its C-terminus

A key function of the C-terminal domain of Rad52 involves its interaction with Rad51, since the gamma-ray sensitivity of a C-terminal *RAD52* truncation, *rad52-327Δ* (*327Δ*), can be partially suppressed by overexpression of Rad51 (48,49). Surprisingly, only two Rad52 protein bands were observed in a *327Δ* mutant strain at any point in the cell cycle (Figure 5D). These truncated bands likely correspond to the 54 and 57 kDa bands seen in wild-type cells. This result suggests that the C terminus of Rad52 is phosphorylated, or alternatively, that Rad52 phosphorylation requires sequences in the C terminus.

Since the Rad51 interaction domain resides in the C terminus, we tested whether this interaction is required

for Rad52 phosphorylation by examining Rad52 protein from *rad52-409-412Δ* (*409-412Δ*), which has a four-amino acid deletion within the C-terminal domain of Rad52 that ablates its interaction with Rad51 (50). In the *409-412Δ* strain, the protein band pattern is identical to wild-type. This result shows that the Rad52–Rad51 interaction is not required for phosphorylation (Figure 5E).

## DISCUSSION

In this study, we analyzed the multiple start codons present in the *S.cerevisiae RAD52* ORF by generating a series of mutations within its N-terminus. We conclude that translation of *RAD52* is initiated from three start codons and each of the resulting protein species are competent in DNA repair and homologous recombination. According to the 'scanning' model (17–20), translation should initiate preferentially when the ribosome encounters the first AUG start site. In the case of *S.cerevisiae RAD52*, the mRNA transcript begins after the second ATG codon (15); therefore, the third ATG codon corresponds to the first translational start site that can be encountered. However, owing to the suboptimal context around the third start site (a T at the −3 position), ribosome slippage at this site likely results in protein expressed from the fourth ATG triplet, which has an optimal A at the −3 position. Alternatively, initiation at the fourth or fifth AUG could be due to shunting or internal ribosome entry [for a review see (51)]. Moreover, the small amount of Rad52 protein synthesized in the *FS4-5* strain suggests that leaky scanning by the ribosomes occurs to bypass start codons three and four and initiate from the fifth (Figure 4, lane 8). By eliminating translation initiation from codons three and four (*E24Stop M34A M38A*), wild-type levels and wild-type activity are seen for Rad52 protein made exclusively from the fifth start codon (Figure 3D; Figure 4, lane 10 and Table 3). The increased gamma-ray resistance of a strain with protein translated only from the fifth start codon (*E24Stop M34A M38A*) compared to the *FS4-5* strain indicates that efficient repair of gamma-ray-induced lesions requires wild-type Rad52 protein levels. This notion is further supported by the observations that a 3- to 4-fold reduction in wild-type Rad52 levels in the *rad52-Y66o SUP4-o* strain results in a 4-fold decrease in spontaneous recombination as well as a 2- to 3-fold increase in gamma-ray sensitivity (Table 3 and data not shown). It was proposed previously that Rad52 protein levels affect heteroallelic recombination more than the repair of gamma-ray-induced lesions (36). However, that conclusion was based on a class of Rad52 mutants (Class D) that contained both a missense mutation as well as decreased protein levels. In light of the results described above, it is likely that protein levels equally affect recombination and repair.

Since the first and second ATG codons are not part of the *RAD52*-encoded mRNA, then the third ATG codon in the *S.cerevisiae RAD52* ORF is the first potential AUG codon in the mRNA. However, for simplicity and consistency with previous work involving various *rad52* mutant strains (36,48–50), throughout this report and in the future, we will continue to number amino acid positions from the first ATG codon based on the *RAD52* ORF predicted by the DNA sequence rather than the first AUG of the *RAD52*-encoded mRNA.

Multiple Rad52 bands are observed where Rad52 can only be translated from either start site three or five (Figure 4, lanes 8–10). Although previous results indicated that protein mobilities of the multiple Rad52 species were not altered after treatment with calf intestinal alkaline phosphatase (45); in this study, we demonstrate that Rad52 protein is indeed phosphorylated and this modification occurs in a cell cycle-independent and cell cycle-dependent manner at serine and/or threonine residues. For example, wild-type cells that are synchronized and released from a G1 arrest exhibit multiple Rad52 bands that after dephosphorylation collapse to a doublet band corresponding to translational products starting from codon three and from codons four and five, which co-migrate (Figure 5C). In addition, both the cell cycle-independent and cell cycle-dependent phosphorylation events require the C terminal domain of Rad52 (Figure 5D), suggesting that Rad52 is phosphorylated at the C terminus. Alternatively, Rad52 may be phosphorylated within the N-terminal domain but its modification requires the presence of the C-terminus. One of the known functions of the C-terminal domain is to interact with Rad51. However, the phosphorylation pattern is not altered by specifically disrupting the Rad52–Rad51 interaction (Figure 5E), suggesting that this interaction, *per se*, is not required for phosphorylation to occur. We, therefore, favor the notion that the C terminus contains phosphorylation targets that function to regulate the interaction between Rad52 and Rad51.

Figure 6 summarizes our interpretation of the pattern of electrophoretic mobilities of Rad52 protein. Unmodified Rad52 translated from the fourth and fifth start codons results in the 54 kDa protein band, which is an unresolved doublet, whereas unmodified Rad52 translated from the third start codon migrates more slowly at 57 kDa (Figure 6A). In $G_1$-arrested wild-type cells, three Rad52 protein bands are detected and they are the result of a combination of unmodified Rad52 species together with a first phosphorylation event (Figure 6B). We suggest that the 57 kDa protein band is a combination of unmodified Rad52 expressed from the third start codon together with additional protein species corresponding to phosphorylated Rad52 translated from the fourth and fifth start codons (Figure 6B, 4* and 5*). Similarly, phosphorylation of Rad52 translated from the third start codon
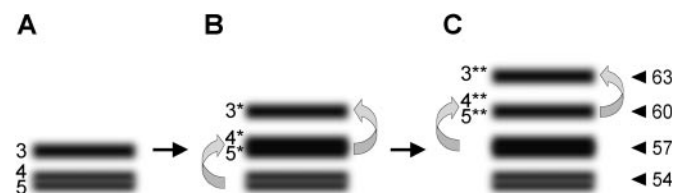


**Figure 6.** Model to explain the multiple Rad52 protein species. (**A**) *RAD52*-encoded mRNA allows protein translation from the third and, by leaky scanning, also from the fourth and fifth start codons (3, 4 and 5, respectively). (**B**) First phosphorylation: cell cycle-independent. Rad52 species from (**A**) (3, 4 and 5) are modified resulting in slower migrating protein species (3*, 4* and 5*, respectively). (**C**) Second phosphorylation: cell cycle-dependent. During S phase, some of 3*, 4* and 5* are modified into 3**, 4** and 5**, respectively. Approximate molecular weights (kDa) corresponding to the observed mobility are indicated.

results in a protein band with slower electrophoretic mobility (60 kDa) (Figure 6B, 3*). Next, we explain the additional 63 kDa Rad52 protein band by a second phosphorylation event occurring in a cell cycle-dependent manner during S phase (Figure 5B; Figure 6C, 3* becoming 3**). This cell cycle regulated phosphorylation event also shifts the intensity of the other species giving rise to 4** and 5**. Thus, we conclude that the substrates for the second modification are the previously phosphorylated Rad52 species.

A possible role for phosphorylation of Rad52 protein may be in the cellular response to DNA damage, where Rad52 relocalizes from a diffuse nuclear distribution to distinct foci at the sites of DSBs (41,52). In fact the appearance of spontaneous Rad52 foci coincides with the cell cycle-dependent phosphorylation [Figure 5C and (43)], suggesting that some aspect of Rad52 focus formation is regulated by phosphorylation. Rad52 phosphorylation is not affected in a $mec1\Delta$ $tel1\Delta$ double mutant, where the two major DNA damage responding kinases are absent (data not shown). This is consistent with the observation that Rad52 phosphorylation is not increased after gamma-irradiation (data not shown). Perhaps the first phosphorylation event that persists throughout the cell cycle is a negative regulator of Rad52 foci and the cell cycle regulated phosphorylation promotes focus formation for homologous recombination.

## ACKNOWLEDGEMENTS

## REFERENCES

1. Resnick,M.A. (1969) Genetic control of radiation sensitivity in *Saccharomyces cerevisiae*. *Genetics*, **62**, 519–531.
2. Game,J.C. and Mortimer,R.K. (1974) A genetic study of x-ray sensitive mutants in yeast. *Mutat. Res.*, **24**, 281–292.
3. Resnick,M.A. and Martin,P. (1976) The repair of double-strand breaks in the nuclear DNA of *Saccharomyces cerevisiae* and its genetic control. *Mol. Gen. Genet.*, **143**, 119–129.
4. Game,J.C., Zamb,T.J., Braun,R.J., Resnick,M. and Roth,R.M. (1980) The role of radiation (rad) genes in meiotic recombination in yeast. *Genetics*, **94**, 51–68.
5. Malone,R.E. and Esposito,R.E. (1980) The *RAD52* gene is required for homothallic interconversion of mating types and spontaneous mitotic recombination in yeast. *Proc. Natl Acad. Sci. USA*, **77**, 503–507.
6. Paques,F. and Haber,J.E. (1999) Multiple pathways of recombination induced by double-strand breaks in *Saccharomyces cerevisiae*. *Microbiol. Mol. Biol. Rev.*, **63**, 349–404.
7. Petes,T.D., Malone,R.E. and Symington,L.S. (1991) Recombination in yeast. In J.R.P.a.E.W.J. J. R,Broach (ed.), *The Molecular and Cellular Biology of the Yeast Saccharomyces: Genome Dynamics, Protein Synthesis and Energetics*.. Cold Spring Harbor Laboratory Press, Cold Spring Harbor, NY, pp. 407–521.
8. Orr-Weaver,T.L., Szostak,J.W. and Rothstein,R.J. (1981) Yeast transformation: a model system for the study of recombination. *Proc. Natl Acad. Sci. USA*, **78**, 6354–6358.
9. Bendixen,C., Sunjevaric,I., Bauchwitz,R. and Rothstein,R. (1994) Identification of a mouse homologue of the *Saccharomyces cerevisiae* recombination and repair gene, *RAD52*. *Genomics*, **23**, 300–303.
10. Bezzubova,O.Y., Schmidt,H., Ostermann,K., Heyer,W.D. and Buerstedde,J.M. (1993) Identification of a chicken RAD52 homologue suggests conservation of the RAD52 recombination pathway throughout the evolution of higher eukaryotes. *Nucleic Acids Res.*, **21**, 5945–5949.
11. Muris,D.F., Bezzubova,O., Buerstedde,J.M., Vreeken,K., Balajee,A.S., Osgood,C.J., Troelstra,C., Hoeijmakers,J.H., Ostermann,K., Schmidt,H. *et al.* (1994) Cloning of human and mouse genes homologous to *RAD52*, a yeast gene involved in DNA repair and recombination. *Mutat. Res.*, **315**, 295–305.
12. Ostermann,K., Lorentz,A. and Schmidt,H. (1993) The fission yeast *rad22* gene, having a function in mating-type switching and repair of DNA damages, encodes a protein homolog to *Rad52* of *Saccharomyces cerevisiae*. *Nucleic Acids Res.*, **21**, 5940–5944.
13. Shen,Z., Denison,K., Lobb,R., Gatewood,J.M. and Chen,D.J. (1995) The human and mouse homologs of the yeast *RAD52* gene: cDNA cloning, sequence analysis, assignment to human chromosome 12p12.2–p13, and mRNA expression in mouse tissues. *Genomics*, **25**, 199–206.
14. Suto,K., Nagata,A., Murakami,H. and Okayama,H. (1999) A double-strand break repair component is essential for S phase completion in fission yeast cell cycling. *Mol. Biol. Cell*, **10**, 3331–3343.
15. Adzuma,K., Ogawa,T. and Ogawa,H. (1984) Primary structure of the RAD52 gene in *Saccharomyces cerevisiae*. *Mol. Cell. Biol.*, **4**, 2735–2744.
16. Carlson,M. and Botstein,D. (1982) Two differentially regulated mRNAs with different 5′ ends encode secreted with intracellular forms of yeast invertase. *Cell*, **28**, 145–154.
17. Kozak,M. (1978) How do eucaryotic ribosomes select initiation regions in messenger RNA? *Cell*, **15**, 1109–1123.
18. Kozak,M. (1986) Point mutations define a sequence flanking the AUG initiator codon that modulates translation by eukaryotic ribosomes. *Cell*, **44**, 283–292.
19. Kozak,M. (1987) At least six nucleotides preceding the AUG initiator codon enhance translation in mammalian cells. *J. Mol. Biol.*, **196**, 947–950.
20. Kozak,M. (1989) The scanning model for translation: an update. *J. Cell Biol.*, **108**, 229–241.
21. Kozak,M. (1984) Compilation and analysis of sequences upstream from the translational start site in eukaryotic mRNAs. *Nucleic Acids Res.*, **12**, 857–872.
22. Cigan,A.M. and Donahue,T.F. (1987) Sequence and structural features associated with translational initiator regions in yeast—a review. *Gene*, **59**, 1–18.
23. Kozak,M. (2002) Pushing the limits of the scanning mechanism for initiation of translation. *Gene*, **299**, 1–34.
24. Kozak,M. (1981) Possible role of flanking nucleotides in recognition of the AUG initiator codon by eukaryotic ribosomes. *Nucleic Acids Res.*, **9**, 5233–5252.
25. Kozak,M. (1984) Selection of initiation sites by eucaryotic ribosomes: effect of inserting AUG triplets upstream from the coding sequence for preproinsulin. *Nucleic Acids Res.*, **12**, 3873–3893.
26. Baim,S.B. and Sherman,F. (1988) mRNA structures influencing translation in the yeast Saccharomyces cerevisiae. *Mol. Cell. Biol.*, **8**, 1591–1601.
27. Yun,D.F., Laz,T.M., Clements,J.M. and Sherman,F. (1996) mRNA sequences influencing translation and the selection of AUG initiator codons in the yeast *Saccharomyces cerevisiae*. *Mol. Microbiol.*, **19**, 1225–1239.
28. Dobson,M.J., Tuite,M.F., Roberts,N.A., Kingsman,A.J., Kingsman,S.M., Perkins,R.E., Conroy,S.C. and Fothergill,L.A. (1982) Conservation of high efficiency promoter sequences in *Saccharomyces cerevisiae*. *Nucleic Acids Res.*, **10**, 2625–2637.
29. Hamilton,R., Watanabe,C.K. and de Boer,H.A. (1987) Compilation and comparison of the sequence context around the AUG start codons in *Saccharomyces cerevisiae* mRNAs. *Nucleic Acids Res.*, **15**, 3581–3593.

30. Kozak,M. (1991) Effects of long 5′ leader sequences on initiation by eukaryotic ribosomes *in vitro*. *Gene Expr.*, **1**, 117–125.

31. Kozak,M. (1991) A short leader sequence impairs the fidelity of initiation by eukaryotic ribosomes. *Gene Expr.*, **1**, 111–115.

32. Kozak,M. (1990) Downstream secondary structure facilitates recognition of initiator codons by eukaryotic ribosomes. *Proc. Natl Acad. Sci. USA*, **87**, 8301–8305.

33. Sherman,F., Fink,G.R. and Hicks,J.B. (1989) *Methods in Yeast Genetics*. Cold Spring Harbor Laboratory Press, Cold Spring Harbor, NY.

34. Thomas,B.J. and Rothstein,R. (1989) Elevated recombination rates in transcriptionally active DNA. *Cell*, **56**, 619–630.

35. Zou,H. and Rothstein,R. (1997) Holliday junctions accumulate in replication mutants via a RecA homolog-independent mechanism. *Cell*, **90**, 87–96.

36. Mortensen,U.H., Erdeniz,N., Feng,Q. and Rothstein,R. (2002) A molecular genetic dissection of the evolutionarily conserved N terminus of yeast *Rad52*. *Genetics*, **161**, 549–562.

37. Erdeniz,N., Mortensen,U.H. and Rothstein,R. (1997) Cloning-free PCR-based allele replacement methods. *Genome Res.*, **7**, 1174–1183.

38. Christianson,T.W., Sikorski,R.S., Dante,M., Shero,J.G. and Hieter,P. (1992) Multifunctional yeast high-copy-number shuttle vectors. *Gene*, **110**, 119–122.

39. Smith,J. and Rothstein,R. (1995) A mutation in the gene encoding the Saccharomyces cerevisiae single-stranded DNA-binding protein Rfa1 stimulates a *RAD52*-independent pathway for direct-repeat recombination. *Mol. Cell. Biol.*, **15**, 1632–1641.

40. Lea,D.E. and Coulson,C.A. (1949) The distribution in the numbers of mutants in bacterial populations. *J. Genet.*, **49**, 264–285.

41. Lisby,M., Rothstein,R. and Mortensen,U.H. (2001) Rad52 forms DNA repair and recombination centers during S phase. *Proc. Natl Acad. Sci. USA*, **98**, 8276–8282.

42. Mortensen,U.H., Bendixen,C., Sunjevaric,I. and Rothstein,R. (1996) DNA strand annealing is promoted by the yeast Rad52 protein. *Proc. Natl Acad. Sci. USA*, **93**, 10729–10734.

43. Lisby,M., Antúnez de Mayolo,A., Mortensen,U.H. and Rothstein,R. (2003) Cell cycle-regulated centers of DNA double-strand break repair. *Cell Cycle*, **2**, 479–483.

44. Shinohara,A., Shinohara,M., Ohta,T., Matsuda,S. and Ogawa,T. (1998) Rad52 forms ring structures and co-operates with RPA in single-strand DNA annealing. *Genes Cells*, **3**, 145–156.

45. Sung,P. (1997) Function of yeast Rad52 protein as a mediator between replication protein A and the Rad51 recombinase. *J. Biol. Chem.*, **272**, 28194–28197.

46. Kunz,B.A., Henson,E.S., Karthikeyan,R., Kuschak,T., McQueen,S.A., Scott,C.A. and Xiao,W. (1998) Defects in base excision repair combined with elevated intracellular dCTP levels dramatically reduce mutation induction in yeast by ethyl methanesulfonate and *N*-methyl-*N*′-nitro-*N*-nitrosoguanidine. *Environ. Mol. Mutagen.*, **32**, 173–178.

47. Wang,S.S. and Hopper,A.K. (1988) Isolation of a yeast gene involved in species-specific pre-tRNA processing. *Mol. Cell. Biol.*, **8**, 5140–5149.

48. Asleson,E.N., Okagaki,R.J. and Livingston,D.M. (1999) A core activity associated with the N terminus of the yeast RAD52 protein is revealed by RAD51 overexpression suppression of C-terminal rad52 truncation alleles. *Genetics*, **153**, 681–692.

49. Milne,G.T. and Weaver,D.T. (1993) Dominant negative alleles of RAD52 reveal a DNA repair/recombination complex including Rad51 and Rad52. *Genes Dev.*, **7**, 1755–1765.

50. Krejci,L., Song,B., Bussen,W., Rothstein,R., Mortensen,U.H. and Sung,P. (2002) Interaction with Rad51 is indispensable for recombination mediator function of Rad52. *J. Biol. Chem.*, **277**, 40132–40141.

51. Hellen,C.U. and Sarnow,P. (2001) Internal ribosome entry sites in eukaryotic mRNA molecules. *Genes Dev.*, **15**, 1593–1612.

52. Lisby,M., Mortensen,U.H. and Rothstein,R. (2003) Colocalization of multiple DNA double-strand breaks at a single Rad52 repair centre. *Nature Cell Biol.*, **5**, 572–577.